CARBON letters

Original Articles
Carbon Letters Vol. 27, 90-97 (2018)

Detection of electromagnetic interference shielding effect of Hanji mixed with carbon nanotubes using nuclear magnetic resonance techniques

Young Seok Byun[1,2], Shin Ae Chae[1], Geun Yeong Park[3], Haeseong Lee[3,♠] and Oc Hee Han[1,2,4,♠]

[1]Western Seoul Center, Korea Basic Science Institute, Seoul 03759, Korea
[2]Graduate School of Analytical Science & Technology, Chungnam National University, Daejeon 34134, Korea
[3]Department of Carbon and Advanced Nanomaterials Engineering, Jeonju University, Jeonju 55069, Korea
[4]Department of Chemistry & Nano Science, Ewha Womans University, Seoul 03760, Korea

Article Info

Received 12 November 2017
Accepted 30 December 2017

♠Corresponding Author
E-mail: haeseong@jj.ac.kr
ohhan@kbsi.re.kr
Tel: +82-2-6908-6220

Open Access

DOI: http://dx.doi.org/10.5714/CL.2018.27.090

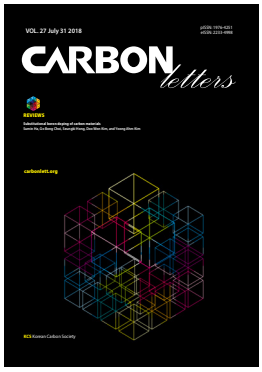

http://carbonlett.org

pISSN: 1976-4251
eISSN: 2233-4998

Abstract

Electromagnetic interference (EMI) shielding is an important issue in modern daily life due to the increasing prevalence of electronic devices and their compact design. This study estimated EMI-shielding effect (EMI-SE) of small (8–14×17 mm) Hanji (Korean traditional paper) doped with carbon nanotubes (CNTs) and compared to Hanji without CNT using ^{2}H (92.1 MHz) and ^{23}Na (158.7 MHz) nuclear magnetic resonance (NMR) peak area data obtained from 1 M NaCl in D_2O samples in capillary tubes that were wrapped in the Hanji samples. The simpler method of using the variation of reflected power and tuning frequency by inserting the sample into an NMR coil was also tested at 242.9, 158.7, and 92.1 MHz. Overall, EMI shielding was relatively more effective at the higher frequencies. Our results validated that NMR methods to be useful to evaluate EMI-SE, particularly for small, flexible shielding materials, and demonstrated that EMI shielding by absorption is dominant in Hanji mixed with CNT.

Key words: carbon nanotubes, electromagnetic interference shielding, nuclear magnetic resonance spectroscopy, Hanji

1. Introduction

Electronic devices such as, television sets, mobile phones, personal computers, and laptops are ubiquitous in modern daily life. As the technology improves, devices have become compact, wireless, and remote controllable for more diverse functions. This raises the requirement to shield parts within devices as well as the overall electronic devices to maintain reliable functionality by removing electromagnetic interference (EMI) from the unwanted sources. Consequently, EMI shielding is an important issue in modern daily life. Generally, EMI shielding has two major mechanisms: reflection and absorption [1-4]. Metals, such as copper, silver, gold, and aluminum mainly shield EMI via reflection due to their conducting electrons [1,2]. However, EMI is more strongly shielded by absorption for larger dielectric constant materials such as $BaTiO_3$, or higher magnetic permeability materials such as Fe_3O_4 [1,2].

Metals have been the preferred materials for EMI shielding, even with disadvantages of high density, corrosion, high cost, and difficulty to improve their mechanical properties [5]. However, these problems can be overcome by light carbon materials with high electrical conductivity, good thermal stability, and flexibility [3,5]. In particular, composite materials that include carbon, such as carbon nanotube (CNT)-polymer composites [3], colloidal graphite [6], and flexible graphite [7] have been proposed for EMI shielding. However, homogeneous distribution of carbon materials has been an issue. Fluorination of carbon black

in electrospun carbon fibers was demonstrated to improvecarbon black dispersion and reduce adhesion between carbon black and carbon fibers [5].

Hanji (Korean traditional paper) has advantages of high durability, good mechanical strength, and there have been several efforts to improve its physical properties and dyeability [8-10]. Therefore, this study prepared Hanji mixed with CNT for EMI shielding. The EMI-shielding effect (EMI-SE) is normally measured in an open field or free space, shielded box, coaxial transmission line, or shielded room [4,11-13]. However, relatively large samples are required and include frequencies ≥1 GHz, although ASTM D4935-10, a widely used US standard for EMI-SE measurement, covers 30 MHz to 1.5 GHz [4,12]. To the best of our knowledge, this study employed nuclear magnetic resonance (NMR) spectroscopy at 92.1, 158.7, and 242.9 MHz for the first time to estimate EMI-SE of relatively small (≤ 2.4 cm^2) flexible Hanji samples placed in a magnetic field (14.1 T).

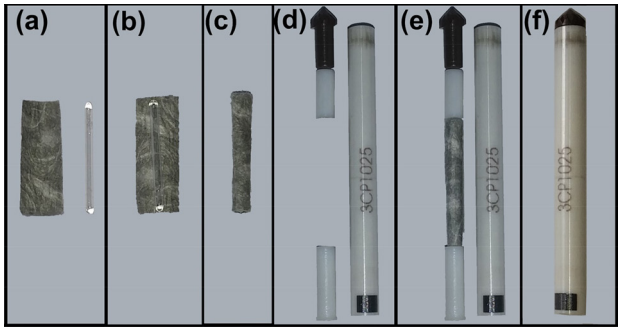

Fig. 1. Sample preparation procedure for NMR experiments: (a) 8×17 mm Hanji sample and capillary tube filled with 2 M NaCl solution in D_2O, (b) capillary tube on top of the Hanji sample, (c) capillary tube wrapped in the Hanji sample, (d) disassembled magic angle spinning (MAS) rotor components, (e) capillary wrapped in Hanji sample and disassembled MAS rotor components aligned, and (f) capillary wrapped in Hanji sample inside the assembled rotor.

2. Experimental

2.1. Preparation and characterization of Hanji with CNT

CNT solutions were prepared by mixing 400 mg sodium dodecyl sulfate (Sigma-Aldrich Co. LLC, USA), and 800 mg single-wall CNT (1.4–1.7 nm diameter, 5–20 μm length, and 95 wt% purity; SA230; Nanosolution Co. Ltd., Korea) with 400 mL deionized water, and sonicating the solution for 1 h to ensure good CNT dispersal.

Hanji samples were prepared by mixing 1.3 g of dried mulberry fiber (Jeonju Traditional Hanji Center, Korea) with 2500 mL of deionized water and stirring the solution using magnetic stirrers until the fiber was well dispersed. Five 500 mL Hanji solutions were mixed with 0, 40, 80, 120, and 160 mL of dispersed CNT solution and 0, 80, 160, 240, or 320 mg of polyacrylamide (PAM), (Choongrim Industrial Co. Ltd., Korea), respectively, while magnetically stirring, producing samples Hanji-1 to Hanji-5, respectively. Each solution mixture was evenly spread over 15×15 cm (225 cm^2) metal frame and dried at 100°C for 30 min.

Thickness and surface resistivity of Hanji samples were measured with a digital micrometer (MDC-25PJ, Mitutoyo Corp., Japan) and resistivity meter (MCP-T610, Mitsubishi Chemical Analytech Co. Ltd., Japan), respectively. CNT content embedded in each Hanji sample was measured as weight percentage using a thermogravimetric analyzer (TGA N-1500, Scinco Co. Ltd., Korea).

2.2. NMR experiments

2.2.1. NMR probe tuning and matching parameters

All NMR experiments were performed with a Varian INOVA 600 MHz NMR spectrometer in a 14.1 T magnetic field using NMR rotors with 5 mm outer diameter. EMI-SE values of Hanji samples were first estimated from tuning values on the tuning stand and/or analyzing wobbling curves. Hanji samples were

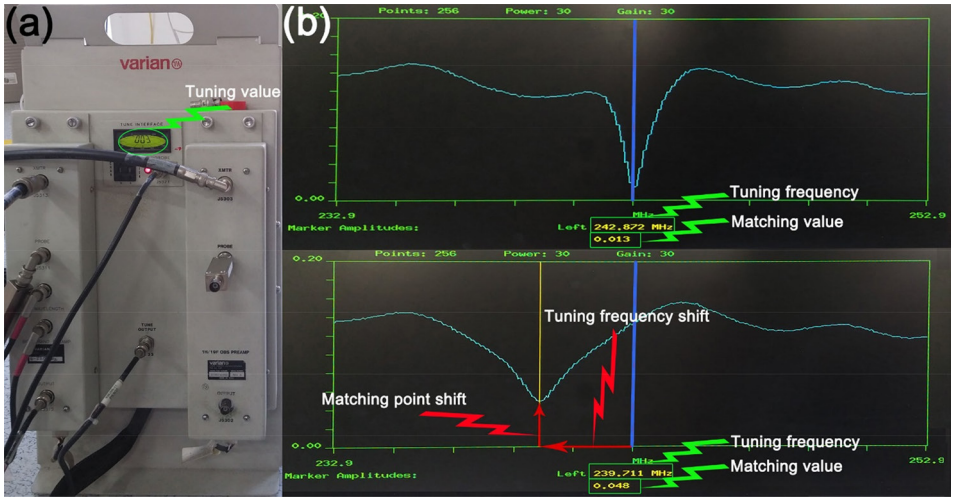

Fig. 2. (a) Tuning value on the tuning stand, and (b) wobbling curves on the NMR instrument monitor for (top) Hanji-1 sample, tuned, and (bottom) Hanji-n sample retaining Hanji-1 tuning where n=2, 3, 4, or 5.

Table 1. Hanji sample properties

Property	Sample				
	Hanji-1	Hanji-2	Hanji-3	Hanji-4	Hanji-5
Amount of CNT solution (mL)[a)]	0	40	80	120	160
CNT content in Hanji (wt%)	0	1.53	2.53	3.58	4.34
Average surface resistance (Ω/□)	-	686±285	316±135	133±35	74±25
Average weight (mg)[b)]	15±5	23±7	18±4	32±6	16±5
Average thickness (mm)	0.28	0.42	0.4	0.6	0.35
Average CNT weight in Hanji sample (mg)[b)]	0	0.35±0.11	0.46±0.10	1.15±0.21	0.69±0.22

[a)]Added to 500 mL Hanji solution.
[b)]For 10×17 mm Hanji samples.

cut to 8, 10, 12, or 14×17 mm. For blank EMI shielding data, a capillary wrapped in 8×17 mm Hanji-1, as shown in Fig. 1, was placed in the probe and the tuning value (Tv) was minimized. The wobbling curve (Fig. 2) was centered and the gap between the curve's minimum point and bottom line was minimized by changing the probe's variable capacitors at 242.872 MHz (^{31}P Larmor frequency), 158.706 MHz (^{23}Na Larmor frequency), or 92.099 MHz (^{2}H Larmor frequency). The Hanji-1 sample was then replaced by Hanji-m samples, where m=2, 3, 4, or 5, and the Tv on the tuning stand (Fig. 2a), tuning frequency shift (T), and reflected power matching point shift (M) (Fig. 2b) were measured.

2.2.2. NMR peak area

NMR samples were prepared as shown in Fig. 1. The capillary tube (2.5 mm outer diameter, 17 mm length) was filled with 0.01 mL of 2 M NaCl solution in D_2O and flame sealed. The tube was then wrapped in a Hanji sample and placed into an NMR rotor. After tuning and matching the probe for ^{23}Na and ^{2}H NMR at 158.706 and 92.099 MHz, respectively, ^{23}Na and ^{2}H NMR spectra were acquired with 5 μs (90° pulse) and 4.5 μs (30° pulse) pulse lengths, respectively. Pulse delay time was 20 s, 4 scans were taken for each sample for both ^{23}Na and ^{2}H NMR experiments, and respective line broadenings of 0 and 10 Hz were applied to the NMR data. NMR peak areas were standardized by setting that for the capillary wrapped in 8×17 mm Hanji-1 as 100.

3. Results and Discussion

3.1. Hanji sample properties

Table 1 shows measured Hanji sample properties, and Fig. 3 shows typical sample images. The samples noticeably darken from Hanji-1 to Hanji-5, as CNT content increases. Although the CNT embedded in the Hanji was not linear with the proportion added to the Hanji solution, average surface resistance decreased as Hanji CNT content increased.

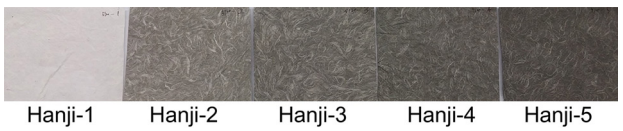

Fig. 3. Typical Hanji sample images.

3.2. NMR results

3.2.1. Tuning and matching parameters

Figs. 4-6 show Tv, T, and M for Hanji samples at 242.872, 158.706, and 92.099 MHz, respectively. The M values are proportional to the reflected radio frequency (RF) power due to impedance mismatch of the probe circuit from 50 Ω, since the circuit impedance was tuned to have zero M at 50 Ω. However, we did not use any unit for the vertical scale because the scale unit for the vertical axis on the particular NMR instrument employed was unclear. On the other hand, the wobbling curve providing the T and M values is commonly used in NMR experiments, and can be monitored on most NMR spectrometers. Even when the wobbling curves were unable to be observed on the NMR spectrometer, a network analyzer could be connected to the spectrometer to monitor them.

Fig. 4 shows that Tv generally increased, T decreased, and M increased with increasing CNT content. However, the largest effect was between Hanji-1 and Hanji-2 samples, with subsequent increased CNT content having significantly less impact. Interestingly, M decreased for increased CNT content for Hanji-3, 4, and 5 samples, that is, maximum shift occurred for Hanji-2. Tv reflect both T and M, and may be simulated as a function of both shifts. For example, the Tv can be approximated by adding the absolute T to M, that is, a(M + |T|) where a=130, 500, and 700, for the three RF frequencies, respectively, as shown in Figs. 4d, 5d, and 6d.

Both M and |T| must be minimized to minimize Tv, which are used as guideline values for probe tuning optimization without watching wobbling curves. T can be positive or negative, whereas M is always positive. Tv can be simulated with various equations, e.g. as shown, or M+bT where b is another proportional constant. Several such equations were assessed and a(M + |T|) had the best fit with experimentally obtained tuning value data.

Hanji length did not influence NMR data although a longer sample resulted in multiple layers when wrapping the capillary. Capping with Hanji at the top and bottom of the Hanji-

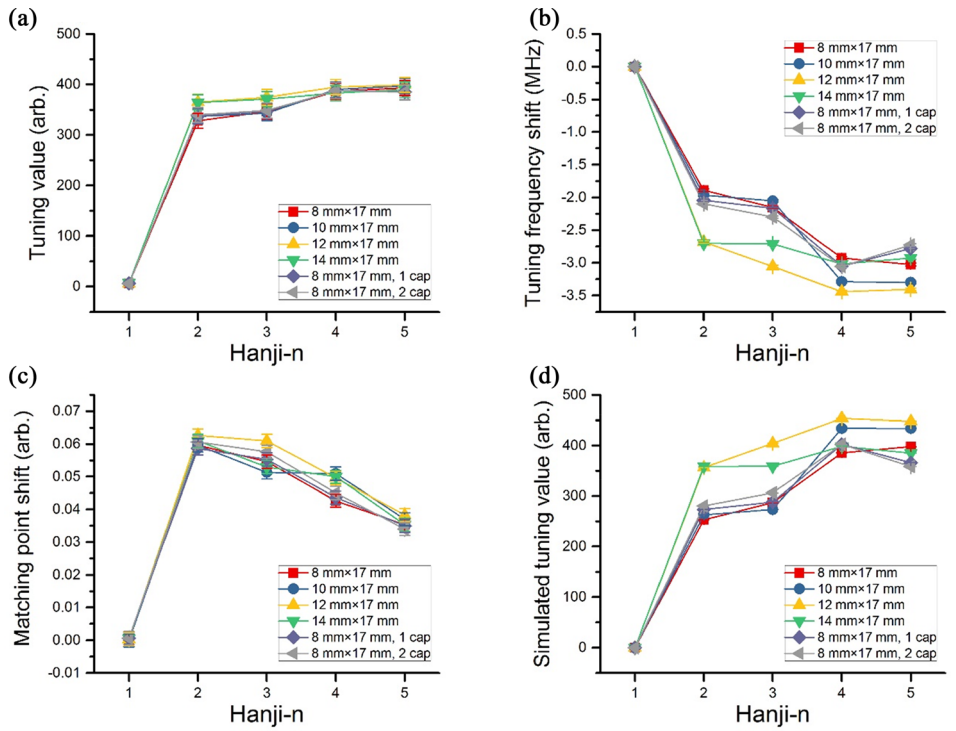

Fig. 4. Hanji-n (n=1, 2, 3, 4, and 5) data at 242.8 MHz under 14.1 T: (a) tuning value, (b) tuning frequency shift, and (c) reflected power matching point shift; and (d) simulated tuning values for constant a=130.

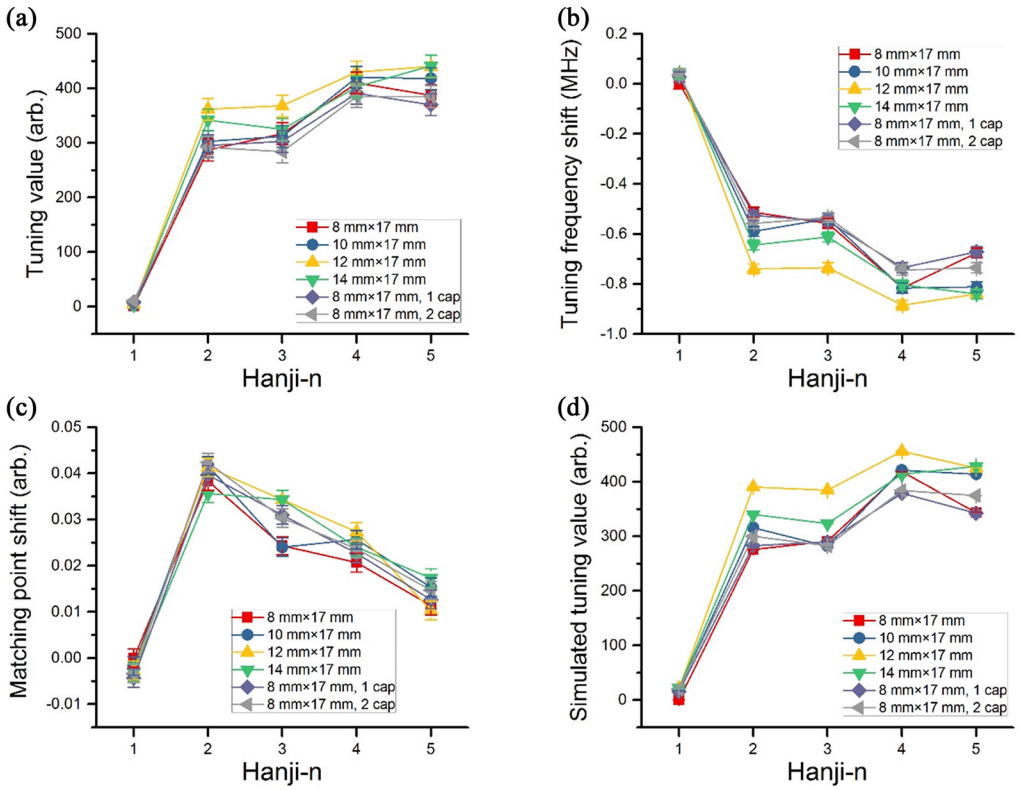

Fig. 5. Hanji-n (n=1, 2, 3, 4, and 5) data at 158.706 MHz under 14.1 T: (a) tuning value, (b) tuning frequency shift, and (c) reflected power matching point shift; and (d) simulated tuning values for constant *a*=500.

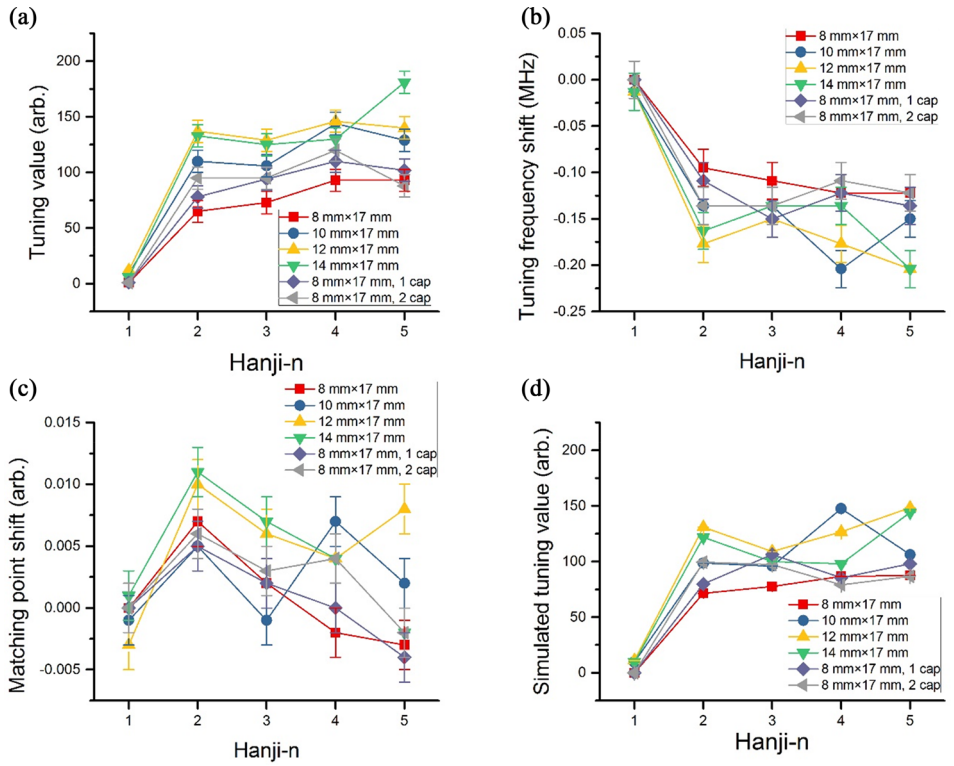

Fig. 6. Hanji-n (n=1, 2, 3, 4, and 5) data at 92.1 MHz under 14.1 T: (a) tuning value, (b) tuning frequency shift, and (c) reflected power matching point shift; and (d) simulated tuning values for constant *a*=700.

roll wrapping the capillary also showed no influence. This insensitivity to capping could be due to much smaller sizes (maximum diameter ~3 mm) compared to the wavelengths (1,234, 1,889, and 3,255 mm at 242.872, 158.706 and 92.099 MHz, respectively) [14]. This overall insensitivity also indicated that EMI-SE was not proportional to CNT content in Hanji, suggesting uneven CNT distribution. It might be practical to smooth the data by averaging data over all doped Hanji samples, for example.

Similar trends were observed for all RFs used in Figs. 5 and 6. The only difference is the variation ranges, with lower RF frequency producing smaller data variation. Consequently, 92.099 MHz data (Fig. 6) look much more scattered than 242.872 MHz data (Fig. 4), but this is an artefact of the relative graph scale. The data trend with CNT content in Hanji was similar for Figs. 4-6.

3.2.2. NMR peak area

Fig. 7 shows ^{23}Na (158.7MHz) and ^{2}H (92.1MHz) NMR peak areas for 2 M NaCl in D_2O wrapped in Hanji samples. The NMR peak area for 8×17 mm Hanji-1 sample was set to 100. Fig. 7a shows that peak areas decreased for Hanji samples with CNT, which was expected from CNT EMI shielding. However, the peak area increased slightly with increased CNT content beyond Hanji-2 even when the Tv for Hanji samples with higher CNT content was larger. The NMR signal for increasing CNT content was expected to reduce under the same experimental conditions, but even with less optimized tuning, the peak areas increased with increasing Hanji CNT content. Therefore, the observation that the peak area of Hanji-2 was minimal in Fig. 7a must be real.

Fig. 7a and b show that Hanji-1 samples have various peak areas for different sizes. Larger or capped Hanji-1 samples exhibit smaller peak areas in ^{23}Na NMR data, as expected, whereas ^{2}H NMR data (Fig. 7b) are somewhat chaotic. Thus, this data variation must be within the experimental error range. Therefore, Fig. 7c and d show the mean peak area over the different lengths and/or a cap for each Hanji-n (n=1, 2, 3, 4, and 5). As observed in NMR M data, peak area is minimal for Hanji-2, and shows smaller variation at lower frequencies.

3.2.3. EMI-SE estimation

EMI-SE was calculated as [15,16]

$$\text{EMI-SE (dB)} = 10 \log(P_o/P_t) \quad (1)$$

, where EMI-SE units are dB; and P_o and P_t are the incident and transmitted electromagnetic power, respectively. P_o and P_t can be substituted with the peak areas of Hanji-1 and Hanji-m, respectively, assuming EMI-SE of Hanji-1 was negligible (P_o = P_t for 8×17 mm Hanji-1). Fig. 8a and b show that the maximum EMI-SE calculated from peak areas was 0.3 dB and 1.6 dB for ^{2}H and ^{23}Na Larmor frequencies, respectively. This confirms that there was was larger EMI-SE at higher frequency, even under 14.1 T. Likewise, Fig. 8c and d show EMI-SE values calculated with P_o and P_t being the inverse Tv of 8×17 mm Hanji-1 and

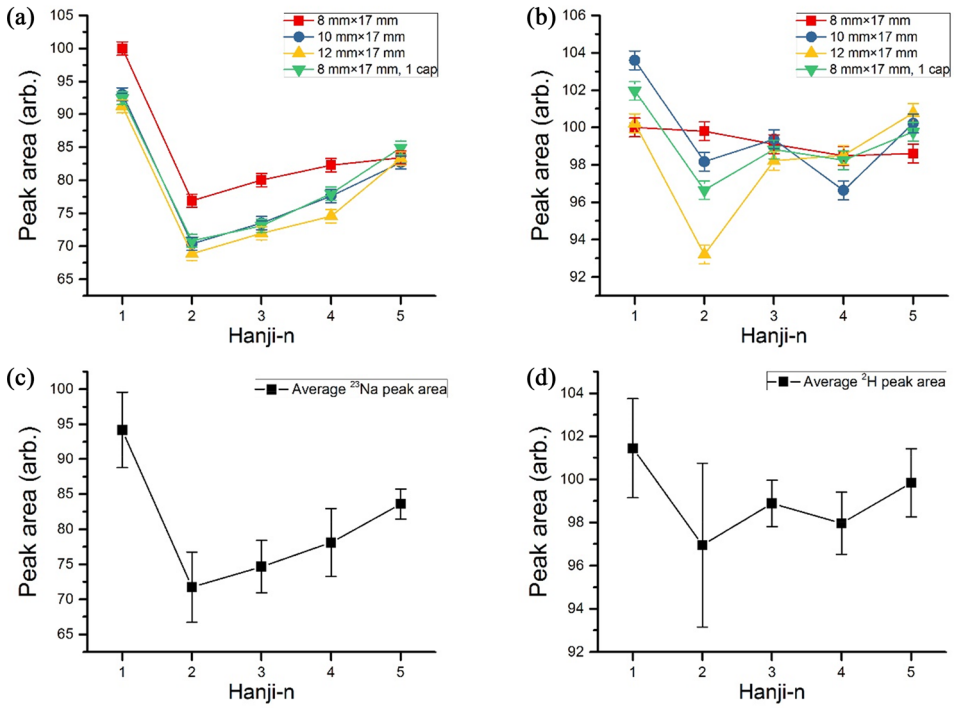

Fig. 7. NMR peak areas of 2 M NaCl in D_2O wrapped in Hanji-n samples (n=1, 2, 3, 4, and 5) for (a) ^{23}Na (158.7 MHz), and (b) ^{2}H (92.1 MHz); and mean NMR peak areas over Hanji sample sizes for (c) ^{23}Na (158.7 MHz), and (d) ^{2}H (92.1 MHz).

Hanji-m (m=2, 3, 4, and 5), respectively. The inverse values were used because Tv decrease for materials with smaller EMI-SE. EMI-SE estimated from tuning values was more sensitive to Hanji-1 size differences.

In NMR spectroscopy, awhen a magnetic field (B_0) is applied, RF (f_0) is determined from Larmor's equation

$$f_0 = \gamma B_0 \tag{2}$$

, where γ is the gyromagnetic ratio of nuclei. NMR signals of given nuclei are known to be proportional to γ^3, which includes the influence of the magnetic field strength applied to and the sensitivity of the NMR detection coil [17]. Therefore, the signal is reduced if the effective magnetic and/or RF field strength at the sample site are decreased due to EMI-SE. RF strength at the sample site is also reduced by the impedance mismatch of the probe due to non-optimized tuning and matching. This study employed 14.1 T magnetic field and RF=158.706 and 92.099 MHz to detect ^{23}Na and ^{2}H nuclei, respectively, to measure EMI-SE at each frequency. NMR peak areas must reflect both magnetic and RF shielding effects in addition to probe impedance mismatch. As discussed above, impedance mismatch generally increased with increasing CNT content in Hanji, which should have reduced peak areas due to the reduced RF field strength at the NaCl in D_2O solution site. However, the experimental data showed the opposite effect, suggesting that the influence of impedance mismatch was negligible compared to magnetic and RF field shielding effects.

Alternatively, peak area variation among Hanji-m samples could be within the experimental range. In this case, EMI-SE can be directly detected from NMR peak area, and increases for increasing frequency. However, the NMR peak area measurements could not distinguish EMI shielding due to CNT content variations in Hanji.

In contrast to peak area, Tv, T, and M data were unaffected by how well the probe was re-tuned and re-matched after Hanji-1 was replaced by Hanji-m samples, because the probe was not re-tuned and only the probe's perturbed state was estimated after replacing the sample.

Increased variation of EMI-SE estimated from Tv or T and M data at higher frequencies may be explained from reflection and absorption loss [18],

$$R_E = 321.8 + 10\log\frac{\sigma}{f_1^3 r^2 \mu}, \tag{3}$$

$$R_H = 14.6 + 10\log\frac{f_1 r^2 \sigma}{\mu}, \tag{4}$$

$$R_P = 168 - 10\log\frac{f_1 \mu}{\sigma}, \tag{5}$$

and

$$A = 131 t\sqrt{f_2 \mu \sigma}, \tag{6}$$

where R_E, R_H, and R_P are the reflection loss for an electric, magnetic, and plane wave field expressed in dB; f_1 and f_2 are frequencies in Hz and MHz, respectively; μ is relative permeability referring to copper; σ is relative conductivity referring to copper; t is the thickness of the shielding materials expressed in mm; r is the distance from the shielding materials to the source expressed

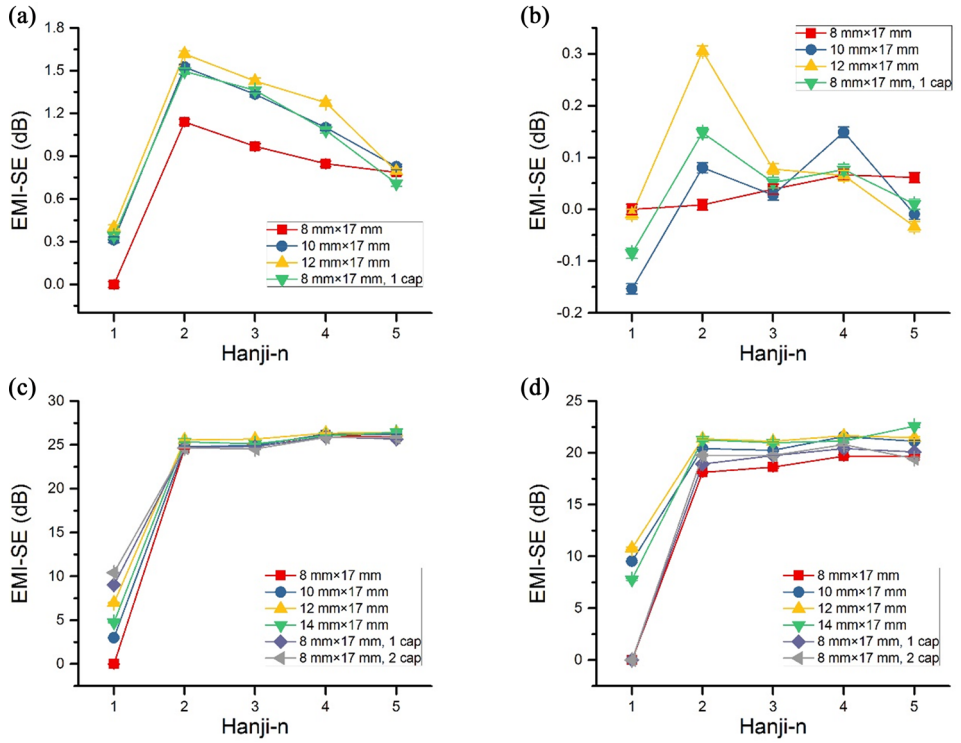

Fig. 8. EMI-SE of 2 M NaCl in D_2O wrapped in Hanji-n (n=1, 2, 3, 4, and 5) calculated from peak areas for (a) ^{23}Na (158.7 MHz), and (b) ^{2}H (92.1 MHz); and calculated from turning values for (c) ^{23}Na and (d) ^{2}H.

in m; A is the absorption loss. Eq. 6 shows that absorption loss is larger at higher frequencies and EMI-SE of Hanji samples doped with CNT is predominantly by absorption. For CNT, μ=4 and σ=0.3355 [19], and μ and σ for the CNT doped Hanji samples may be treated as a function of those depending on actual CNT content.

Generally, it is very difficult to measure EMI-SE of magnetic field with conventional methods. For example, ASTM D4935-10 measures only electric field components, E_x and E_y among the 6 electric and magnetic fields components since it is conducted under far-field condition. With the advent of wearable electronic devices, new methods are urgently required to evaluate the EMI-SE at both far and near field, including those of E_z and the whole magnetic field. Although ASTM D4935-10 can be adapted for near field measurements, another method is required to confirm the EMI-SE data, particularly under static electromagnetic field. The innovative methods demonstrated in this study may provide a good complimentary approach to conventional methods

4. Conclusions

This study developed several methods to measure EMI-SE using relatively simple NMR techniques, which are complimentary to conventional methods, such as ASTM D4935-10. EMI-SE from CNT doped Hanji was estimated at a few tens to a few hundred MHz RF under 14.1 T using NMR peak area reduction. Tuning values, tuning frequency shifts, and reflected power matching point shifts were also employed to estimate EMI-SE without requiring NMR data. The latter method has the advantage of not requiring expensive NMR instruments.

The results showed that EMI-SE from CNT doped Hanji samples were larger at higher frequencies, which implies the shielding mode is predominantly absorption. However, CNT distribution in the Hanji samples was inhomogeneous, resulting in considerable data variation, particularly at lower frequencies. Future studies will correlate EMI-SE data with measured CNT content and distribution in Hanji.

This study measured RF and magnetic field shielding effects simultaneously at a fixed magnetic field strength. Future studies will investigate various magnetic field strengths to identify the influence of magnetic fields on EMI shieling in conjunction with RF. This additional information will provide EMI-SE data in matrix form, and is currently in progress. Quantitative comparisons of EMI-SE data with standard method measurements will also be investigated.

Conflict of Interest

No potential conflict of interest relevant to this article was reported.

Acknowledgements

This work was supported by the National Science and Technology Council Grant (DRC-14-1-KBSI).

References

[1] Chung DDL. Materials for electromagnetic interference shielding. J Mater Eng Perform, **9**, 350 (2000). https://doi.org/10.1361/105994900770346042.

[2] Chung DDL. Electromagnetic interference shielding effectiveness of carbon materials. Carbon, **39**, 279 (2001). https://doi.org/10.1016/S0008-6223(00)00184-6.

[3] Al-Saleh MH, Sundararaj U. Electromagnetic interference shielding mechanisms of CNT/polymer composites. Carbon, **47**, 1738 (2009). https://doi.org/10.1016/j.carbon.2009.02.030.

[4] Geetha S, Kumar KKS, Rao CRK, Vijayan M, Trivedi DC. EMI shielding: methods and materials-a review. J Appl Polym Sci, **112**, 2073 (2009). https://doi.org/10.1002/app.29812.

[5] Im JS, Kim JG, Lee YS. Fluorination effects of carbon black additives for electrical properties and EMI shielding efficiency by improved dispersion and adhesion. Carbon, **47**, 2640 (2009). https://doi.org/10.1016/j.carbon.2009.05.017.

[6] Cao J, Chung DDL. Colloidal graphite as an admixture in cement and as a coating on cement for electromagnetic interference shielding. Cem Concr Res, **33**, 1737 (2003). https://doi.org/10.1016/S0008-8846(03)00152-2.

[7] Luo X, Chung DDL. Electromagnetic interference shielding reaching 130 dB using flexible graphite. Carbon, **34**, 1293 (1996). https://doi.org/10.1016/0008-6223(96)82798-9.

[8] Seo YB, Kim YW, Lee MW, Jung SY. Improvements in the physical properties of Hanji by using red algae pulp. J Korea TAPPI, **41**, 33 (2009).

[9] Yoo SI, Oh UM, Min YR, Choi TH. Improvement on dyeability of Hanji with natural dyes using a (3-chloro-2-hydroxypropyl) trimethyl ammonium chloride. J Korea TAPPI, **43**, 88 (2011).

[10] Kim KJ, Lee MH, Eom TJ. Strengthening treatment of aged Hanji with solvent soluble polymers. J Korea TAPPI, **44**, 1 (2012). https://doi.org/10.7584/ktappi.2012.44.1.001.

[11] Vavrda M, Hertl I. Automatic measurement of small boxes shielding effectiveness. Meas Sci Rev, **6**, 22 (2006).

[12] Li Y, Chen C, Zhang S, Ni Y, Huang J. Electrical conductivity and electromagnetic interference shielding characteristics of multiwalled carbon nanotube filled polyacrylate composite films. App Surf Sci, **254**, 5766 (2008). https://doi.org/10.1016/j.apsusc.2008.03.077.

[13] Dřínovský J, Kejík Z. Electromagnetic shielding efficiency measurement of composite materials. Meas Sci Rev, **9**, 109 (2009). https://doi.org/10.2478/v10048-009-0020-8.

[14] Chase B, Citterio M, Lanni F, Makowiecki D, Radeka V, Rescia S, Takai H, Ban J, Parsons J, Sippach W. Characterization of the coherent noise, electromagnetic compatibility and electromagnetic interference of the ATLAS EM calorimeter front end board, in Proceedings of 5th Conference on Electronics for LHC Experiments (LEB 99), Snowmass, CO, 222 (1999).

[15] Maiti S, Shrivastava NK, Suin S, Khatua BB. Polystyrene/MWCNT/graphite nanoplate nanocomposites: efficient electromagnetic interference shielding material through graphite nanoplate−MWCNT−graphite nanoplate networking. ACS Appl Mater Interfaces, **5**, 4712 (2013). https://doi.org/10.1021/am400658h.

[16] Lee CY, Song HG, Jang KS, Oh EJ, Epstein AJ, Joo J. Electromagnetic interference shielding efficiency of polyaniline mixtures and multilayer films. Synth Met, **102**, 1346 (1999). https://doi.org/10.1016/S0379-6779(98)00234-3.

[17] Derome AE. Modern NMR Techniques for Chemistry Research, Pergamon Press, Oxford, 131 (1987).

[18] Tong XC. Advanced Materials and Design for Electromagnetic Interference Shielding, CRC Press, Florida, 14 (2008).

[19] Zhang W, Xiong H, Wang S, Li M, Gu Y. Electromagnetic characteristics of carbon nanotube film materials. Chin J Aeronaut, **28**, 1245 (2015). https://doi.org/10.1016/j.cja.2015.05.002.